ACS APPLIED MATERIALS & INTERFACES

Research Article

www.acsami.org

Selective Protein Separation Using Siliceous Materials with a Trimethoxysilane-Containing Glycopolymer

Hirokazu Seto,[†] Yutaro Ogata,[†] Tatsuya Murakami,[‡] Yu Hoshino,[†] and Yoshiko Miura[†,*]

[†]Department of Chemical Engineering, Graduate School of Engineering, Kyushu University, 744 Motooka, Nishi-ku, Fukuoka 819-0395, Japan.

[‡]Center for Nano Materials and Technology, Japan Advanced Institute of Science and Technology, 1-1 Asahidai, Nomi, Ishikawa 923-1292, Japan.

Supporting Information

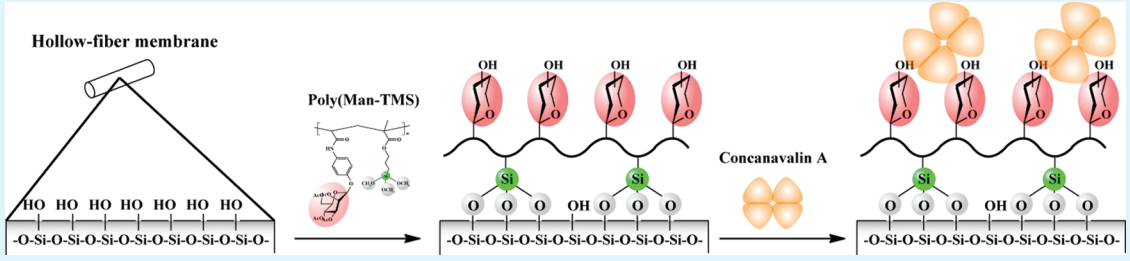

ABSTRACT: A copolymer with α-D-mannose (Man) and trimethoxysilane (TMS) units was synthesized for immobilization on siliceous matrices such as a sensor cell and membrane. Immobilization of the trimethoxysilane-containing copolymer on the matrices was readily performed by incubation at high heat. The recognition of lectin by poly(Man-*r*-TMS) was evaluated by measurement with a quartz crystal microbalance (QCM) and adsorption on an affinity membrane, QCM results showed that the mannose-binding protein, concanavalin A, was specifically bound on a poly(Man-*r*-TMS)-immobilized cell with a higher binding constant than bovine serum albumin. The amount of concanavalin A adsorbed during permeation through a poly(Man-*r*-TMS)-immobilized membrane was higher than that through an unmodified membrane. Moreover, the concanavalin A adsorbed onto the poly(Man-*r*-TMS)-immobilized membrane was recoverable by permeation of a mannose derivative at high concentration.

KEYWORDS: *surface modification, silane coupling reagent, glycopolymer, lectin, QCM, membrane*

1. INTRODUCTION

It is known that saccharides on cell surfaces are involved in various biological phenomena, such as protein binding, cell adhesion, and pathogen infection.[1] Conjugation of saccharides with materials enables molecular recognition and the development of artificial materials on which biological phenomena can be carried out in vitro. Although the molecular recognition ability of monovalent saccharides is relatively weak for use as biomaterials, the saccharide−protein interaction can be amplified by multivalency, known as the glyco-cluster effect.[2,3] We have described various glycopolymers with high affinities for proteins and pathogens.[4−18]

One of the aims of glycopolymer applications is the fabrication of biological devices using the molecular recognition ability of saccharides. Because saccharides have affinities as ligands for various pathogens, including toxic proteins,[19] viruses,[20] and bacteria,[21] glycopolymers are applicable in bioadhesive or separation devices. Pathogen removal devices are often designed on the basis of the size exclusion mechanism with fine porous materials. The sizes of bacteria are of the order of micrometers; however, those of toxic proteins and viruses are of the order of nanometers. Bacteria are removed by microporous materials, whereas the toxic proteins and viruses can be removed by ultrafine nanoporous materials. However, ultrafiltration suffers from problems of high pressure loss during permeation of biomolecule solutions and cake layer formation (fouling by filtration residues). Some proteins specifically or group-specifically interact with various ligands, including antigen−antibody, enzyme−substrate, lectin−saccharide, amino acid−protein, dye−protein, and metal chelate−protein combinations. Therefore, affinity adsorption is an effective method for bioseparation compared with size exclusion.[22−28] When a membrane structure with through-pores is used, the target biomolecule is quickly driven by convectional flow to the vicinity of the immobilized saccharide. Additionally, pressure loss during permeation of the target solution is decreased because of the microscale pores. These advantages are expected to be applicable in devices used for water purification and hemodialysis.

Immobilization of glycopolymers on materials is necessary for the fabrication of bioseparation devices. Various methods of surface modification have been reported, such as self-assembled

Received: October 25, 2011
Accepted: December 9, 2011
Published: December 9, 2011

 © 2011 American Chemical Society

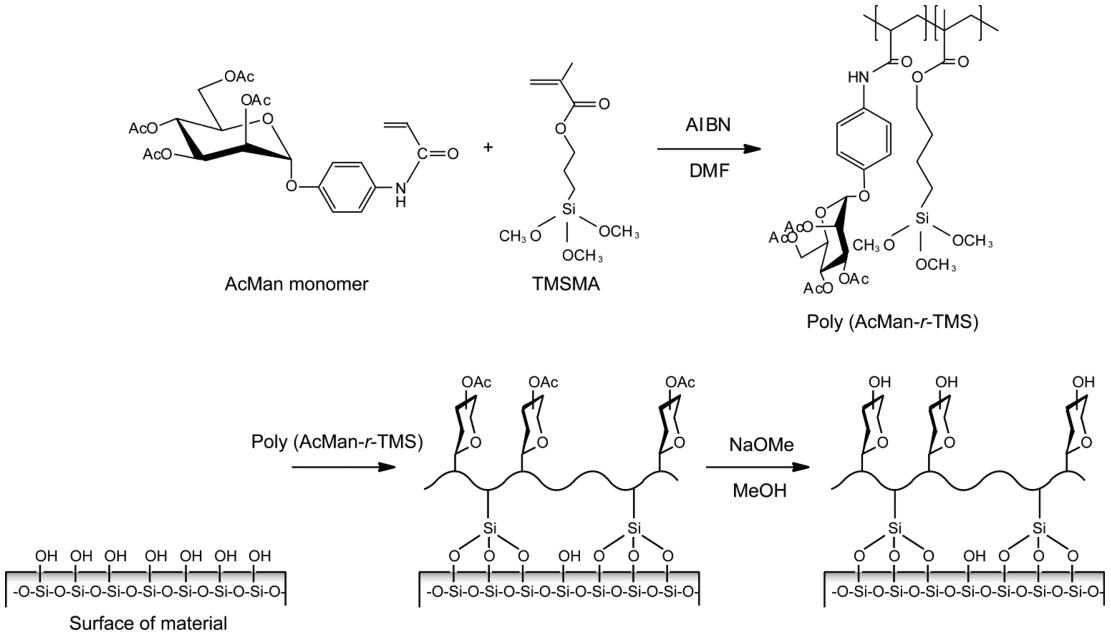

Figure 1. Preparation of poly(Man-*r*-TMS)-immobilized materials.

monolayer formation via Au−S and chemical reactions on substrates,[14,17,18,29,30] though reactions are limited because few functional groups are available. Silica is a useful matrix for bioseparation devices because of its geometric versatility, and glyco-modification of silica has been intensively investigated. Copper-catalyzed cycloaddition between an alkyne and azide groups (click chemistry) has been applied for the preparation of saccharide-immobilized surfaces.[31−34] Formation of isourea bonding is also an effective technique for immobilization of saccharides.[35] Silane coupling reagents have both organic functional groups and hydrolyzable trimethoxysilane groups (TMS). Through the characteristic structure of silane coupling reagents, the TMS moiety is able to form covalent bonds with hydroxyl groups on various matrix surfaces, such as silica glass,[36−43] and also metal oxides[44−48] and cellulose.[39,49−52] Therefore, the silane coupling reagent plays an effective role as a linker between organic compounds and matrices. When a polymerizable silane coupling reagent with a vinyl group, e.g., 3-(trimethoxysilyl) propyl methacrylate (TMSMA), is partially incorporated into a polymer chain together with saccharide units, the surface of the matrix can be directly modified by immobilization of saccharide-containing polymers via TMS moieties in the silane coupling unit.

In this study, a copolymer with α-D-mannose (Man) and TMS as side chains, poly(Man-*r*-TMS), was synthesized for surface modification of a sensor cell and membrane, as shown in Figure 1. The Man and TMS units in poly(Man-*r*-TMS) act as biomolecular-recognition and matrix-binding sites, respectively. Man is an important and major component of the glycochain on the cellular surface, and specifically interacts with various lectins.[53] Lectin recognition by poly(Man-*r*-TMS) immobilized on the surface was investigated using quartz crystal microbalance (QCM). Subsequently, a poly(Man-*r*-TMS)-immobilized membrane device was used for selective separation of lectin; this is applicable to separation of pathogens such as viruses and toxin proteins.

2. EXPERIMENTAL SECTION

2.1. Reagents and Substrates. The following reagents were used as received: D-Mannose (Man) (Tokyo Chemical Industry Co. Ltd., Tokyo, Japan), 3-(trimethoxysilyl) propyl methacrylate (TMSMA), and albumin from bovine serum (BSA) (Sigma Co., St. Louis, MO, USA), 2,2′-azobis isobutyronitrile (AIBN) (Wako Pure Chemical Industries Ltd., Osaka, Japan), and concanavalin A (ConA) (J-Oil Mills Inc., Tokyo, Japan). FITC-I (DOJINDO LABORATORIES, Kumamoto, Japan) and dansyl chloride (Towa Chemical Industry Co. Ltd., Tokyo, Japan) were used for preparation of fluorescent-labeled proteins. A Shirasu porous glass membrane (SPG membrane: Lot No., PEN10J25; effective length, 1.2 cm; average pore diameter, 2100 nm; specific surface area, 1.1 m^2/g) made of silica and alumina was purchased from SPG Technology Co., Ltd., Miyazaki, Japan.

2.2. Synthesis of Poly(AcMan-*r*-TMS). *p*-Acrylamidophenyl 2,3,4,6-tetra-*O*-acetyl-α-D-mannopyranoside (AcMan monomer) was synthesized by a method previously described in the Supporting Information of ref 14. AcMan monomer (255 μmol) and polymerizing inhibitor-free TMSMA (36 μmol) were dissolved in *N*,*N*-dimethylformamide (DMF, 3 mL) anhydride. Polymerization of poly(AcMan-*r*-TMS) was performed in a Schlenk flask. The mixture was degassed using nitrogen gas. The polymeric reaction was initiated by addition of AIBN (6.0 μmol) at 70 °C. After 20 h, the mixture solution was aerated to stop polymerization and the mixture solution was then concentrated by evaporation. Composition and molecular size were determined by hydrogen nuclear magnetic resonance (^{1}H NMR, JNM-ECP400, JEOL Ltd., Tokyo, Japan) and dynamic light scattering (DLS, Zetasizer Nano ZS, Malvern Instruments Ltd., Worcestershire, UK), respectively. The calibration curve for estimation of the hydrodynamic diameter was prepared using polystyrene standards in the molecular weight range 1200−1 280 000 (Showa Denko K. K., Tokyo, Japan, Lot No. 91201).

2.3. Preparation of Poly(Man-*r*-TMS)-Immobilized Sensor Cell and Membrane. To activate the surface of the matrix, we added piranha solution consisting of sulfuric acid and hydrogen peroxide (3:1) dropwise onto a commercially available silica-deposited sensor cell (effective area, 4.9 mm^2) washed with sodium dodecyl sulfate solution, and then rinsed the sensor cell with Milli-Q water (Millipore Corporation, Billerica, MA, USA). This procedure was repeated three times. Poly(AcMan-*r*-TMS) solution in DMF (10 g/L, 1 μL) was added dropwise onto the activated surface and the cell was incubated at 38 and 110 °C for 5 h and 5 min, respectively. Deacetylation of poly(AcMan-*r*-TMS) was carried out by stirring in MeONa (solvent,

dx.doi.org/10.1021/am2014713 | ACS Appl. Mater. Interfaces 2012, 4, 411−417

MeOH; pH ~10; 500 μL) for 30 min. Because TMS cross-links with hydroxyl groups of mannose, deacetylation after the immobilization of the copolymer is recommended. The amount of poly(Man-*r*-TMS) immobilized on the sensor cell was estimated from frequency changes measured by QCM (AFFINIXQ4, Initium Inc., Tokyo, Japan) with a fundamental resonance frequency (F_0) of 27 MHz before and after immobilization treatments. The existence of poly(AcMan-*r*-TMS) on surface was confirmed by X-ray photoelectron spectroscopy (XPS, AXIS-ultra, Shimadzu/Kratos, Kyoto, Japan) using a silicon wafer as the matrix. The contact angles of the poly(AcMan-*r*-TMS)-immobilized silicon wafer before and after deacetylation were measured by the sessile drop method (DropMaster 300, Kyowa Interface Science, Saitama, Japan). The measurements were performed at five spots.

To impregnate poly(AcMan-*r*-TMS) on the SPG membrane, we immersed the membrane in a poly(AcMan-*r*-TMS) solution (THF, 10 g/L, 1.5 mL) at room temperature and 60 °C for 1 and 5 h, respectively. Subsequently, covalent bonding between silanols on the membrane surface and the TMS moiety in the copolymer was formed by heat treatment at 110 °C for 1 h. The amount of poly(AcMan-*r*-TMS) immobilized was estimated from the change in membrane weight. Poly(AcMan-*r*-TMS) immobilized on the membrane was deacetylated using the same method as for the sensor cell. The surface properties of the membrane immobilized with poly(AcMan-*r*-TMS) were evaluated by XPS and scanning electron microscopy (SEM, JSM6701F, JEOL Ltd., Tokyo, Japan).

2.4. Detection of Proteins Using Poly(Man-*r*-TMS)-Immobilized Sensor Cell. The recognition ability of poly(Man-*r*-TMS) on the surface was evaluated by QCM measurements. BSA and Con A were used as protein probes. The poly(Man-*r*-TMS)-immobilized sensor cell was suffused with Ca^{2+} and Mg^{2+}-containing phosphate buffer solution until the frequency reached a steady state. Each protein, at various concentrations, was injected into the sensor cell, and the frequency changes (ΔF) were recorded.

The apparent binding constant (K_a) between poly(Man-*r*-TMS) and Con A and the maximum capacity of the poly(Man-*r*-TMS)-immobilized sensor cell against Con A were estimated from Langmuir's equation as follows:

$$\Delta F = \frac{[\text{lectin}]\Delta F_{\max}}{1/K_a + [\text{lectin}]} \quad (1)$$

The relationship of ΔF to the mass change of protein adsorbed on the surface (Δm) is defined by the Sauerbrey equation[54]

$$\Delta F = -\frac{2NF_0^2}{\sqrt{\rho\mu}}\frac{\Delta m}{A} \quad (2)$$

where N, F_0, ρ, μ, and A are the harmonic overtone, the fundamental resonance frequency, the crystal density, the elastic modulus of the crystal, and the surface area, respectively.

For confirmation of the specificity of the poly(Man-*r*-TMS)-immobilized sensor cell, we added Man with various equivalence molar ratios to Con A solution, and incubated the mixture solutions to prepare Man-pretreated Con A. The solution of Man-pretreated Con A was injected into the sensor cell, and ΔF was recorded to estimate $\Delta F_{\max}$ against Man-pretreated Con A.

2.5. Adsorption of Proteins with Poly(Man-*r*-TMS)-Immobilized Membrane. The recognition ability of poly(Man-*r*-TMS) on the membrane surface was also evaluated by adsorption during permeation of a protein solution. Each protein solution (10 mg/L) feed was passed through the poly(Man-*r*-TMS)-immobilized membrane at 10 mL/h. The effluent was continuously collected and the concentration of protein in the effluent was determined colorimetrically using Bradford reagent.[55] The amount of protein adsorbed on the membrane (q) was calculated from the following equation

$$q\ (\text{nmol/m}^2) = \int_0^v \frac{C_f - C_e}{A}\mathrm{d}v \quad (3)$$

where C_f and C_e are the concentration of protein in the feed and effluent solutions, respectively.

To elute the Con A adsorbed by poly(Man-*r*-TMS) immobilized on the membrane, Milli-Q water and a saturated aqueous solution of *p*-nitrophenyl-α-D-mannoside (*p*NP-Man),[14] which is the intermediate of the AcMan monomer, were permeated through the membrane at 10 mL/h. The effluent was continuously recovered and the concentration of eluted Con A determined using Bradford reagent.

Adsorption of Con A on the poly(Man-*r*-TMS)-immobilized membrane was measured in coexistence with BSA. Con A and BSA was labeled with different fluorescence of FITC-I and dansyl chloride, respectively. The mixture solution of dansyl-Con A (5 mg/L) and FITC-BSA (5 mg/L) was passed through the poly(Man-*r*-TMS)-immobilized membrane at 10 mL/h. The effluent was continuously collected and the concentrations of fluorescent-labeled protein in the effluent were determined using a spectrofluorometer (FP-6500, JASCO Corporation, Tokyo, Japan). The excitation/emission wavelengths of dansyl-Con A and FITC-BSA were 325/515 and 488/520 nm, respectively.

3. RESULTS AND DISCUSSION

3.1. Composition and Molecular Size of Poly(AcMan-*r*-TMS). Poly(AcMan-*r*-TMS) was obtained by free-radical polymerization. The ^{1}H NMR spectrum (see Figure S1 in the Supporting Information) showed that almost all of the monomers disappeared because of no peak corresponded to the vinyl group (δ: 6.2−6.5 ppm). The ratio of AcMan to TMS in the copolymer was estimated to be 85:15 from the integral ratio between the peaks for phenyl group in AcMan (δ: 7.0 ppm, 2H per unit) and the peak for the methoxide group in TMS (δ: 3.5 ppm, 9H per unit). When the amount of TMSMA in the feed monomer increased (AcMan monomer:TMSMA = 50.0:50.0 and 12.5:87.5), peaks corresponding to the vinyl group (δ: 6.2−6.5 ppm) were observed in the ^{1}H NMR spectra (see Figure S2 in the Supporting Information). It is estimated that the feeds with high ratio of TMSMA were not converted, as a result of condensation of silane coupling reagent and termination by fragments cleaved between C and Si in TMSMA.[56]

The molecular sizes of poly(AcMan-*r*-TMS) were estimated by DLS. The size distributions of the AcMan monomer and poly(AcMan-*r*-TMS) in DMF are shown in Figure 2. The

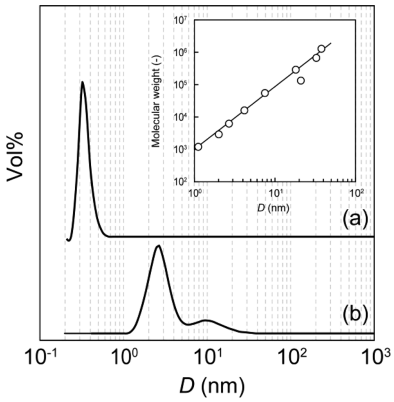

Figure 2. Size distributions of (a) AcMan monomer and (b) poly(AcMan-*r*-TMS) at a concentration of 1 g/L in DMF. The scattergraph in the figure is the calibration curve prepared using polystyrene solutions.

major molecular size of poly(AcMan-*r*-TMS) was 2.7 nm. A small amount of copolymer with 9.7 nm was also detected, indicating that the copolymer aggregated by condensation between TMS units. The larger size of the copolymers

dx.doi.org/10.1021/am2014713 | ACS Appl. Mater. Interfaces 2012, 4, 411−417

compared with the monomers also suggested the progress of the polymerization reaction. From a calibration curve prepared using polystyrene standards, the molecular weight of poly(AcMan-*r*-TMS) was found to be 6200.

3.2. Evaluation of Protein Recognition of Poly(Man-*r*-TMS) Using QCM. The obtained poly(AcMan-*r*-TMS) was immobilized on a silica-deposited cell for QCM detection. The frequency changes indicated that the amount of poly(AcMan-*r*-TMS) immobilized was 16.4 ± 8.4 mg/m^2. Immobilization of poly(AcMan-*r*-TMS) using the silicon substrate was confirmed by XPS (Figure 3). Comparing the C(1s) spectra of

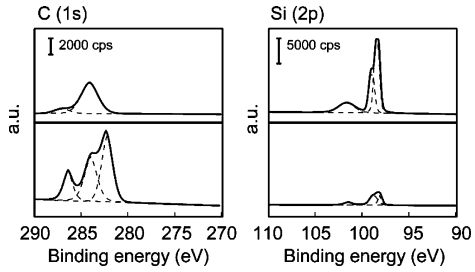

Figure 3. XPS spectra of the silicon surface before and after immobilization of poly (AcMan-*r*-TMS). Above, unmodified silicon; below, poly(AcMan-*r*-TMS)-immobilized silicon.

unmodified and poly(AcMan-*r*-TMS)-immobilized silicon, the peak at 282.2 eV was predominantly detected after immobilization of the copolymer. This peak is related to C−Si bonding of the TMS moiety. Overall, the intensities in Si(2p) of poly(AcMan-*r*-TMS)-immobilized silicon, corresponding to silica and silicon, were weaker than that of unmodified silicon, because the copolymer interfered with X-ray irradiation onto the silicon surface. Therefore, saccharides are immobilizable on a silicon surface via the silane coupling reaction.

The immobilized poly(AcMan-*r*-TMS) was deacetylated using MeONa. The contact angles of water droplet on poly(AcMan-*r*-TMS)-immobilized and deacetylated silicon were measured (see Figure S3 in the Supporting Information), and were 58.1 and 47.7°, respectively. The immobilization of poly(AcMan-*r*-TMS) resulted in an increase in the contact angle, compared with that on the unmodified surface (<30.0°). The deacetylated silicon had a slightly lower contact angle than the poly(AcMan-*r*-TMS)-immobilized silicon because of hydrophilicity. Deacetylation was also confirmed using a soluble AcMan homopolymer. In ^{1}H NMR spectra of an AcMan homopolymer deacetylated under the same conditions as the immobilized copolymer (see Figure S4 in the Supporting Information), the completion of deacetylation reaction was demonstrated by the disappearance of peaks at 1.8−2.2 ppm, corresponding to acetyl groups. This indicated that acetyl groups in the copolymer immobilized on the surface were cleaved.

The specific interaction of poly(Man-*r*-TMS) with Con A was evaluated by QCM using a deacetylated sensor cell. When a protein solution was injected into the sensor cell, a negative ΔF was promptly observed, which eventually reached a steady state. The changes in frequency at steady state as a function of protein concentration are shown in Figure 4. The ΔF of Con A bound on the poly(Man-*r*-TMS)-immobilized cell reached around 2000 Hz, whereas that on the unmodified cell was around 1000 Hz. In contrast, the ΔF of BSA on the poly(Man-*r*-TMS)-immobilized cell was not detectable, whereas that on

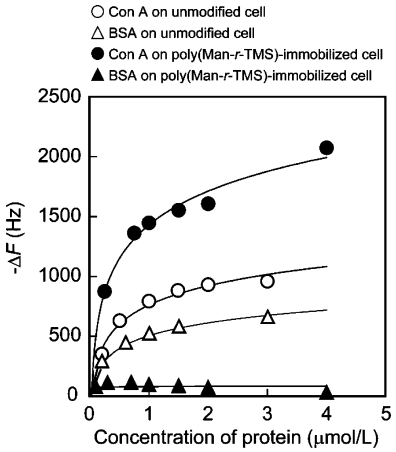

Figure 4. Frequency changes in QCM as a function of the concentration of proteins in unmodified and poly(Man-*r*-TMS)-immobilized cells.

the unmodified substrate reached around 700 Hz. Thus the amount of Con A bound on the poly(Man-*r*-TMS) was almost double that on the unmodified cell, and the amount of BSA bound on the poly(Man-*r*-TMS) was markedly reduced compared with that on the unmodified cell. The results suggest specific and strong adsorption of Con A on poly(Man-*r*-TMS).

The K_a between poly(Man-*r*-TMS) and Con A and the ΔF_{max} of the poly(Man-*r*-TMS)-immobilized sensor cell against Con A, estimated from ΔF using eqs [1] and [2], were 2.5 ± 0.7 × 10^6 M^{-1} and 2110 ± 90 Hz, respectively. The K_a of poly(Man-*r*-TMS) was higher than that of methyl-Man, known to be an inhibitor,[57] with an order of 10^3−10^4 M^{-1} in solution.[58] The higher K_a value of poly(Man-*r*-TMS) shows that Man units on the surface interacted multivalently with Con A. In other words, the glyco-cluster effect of the poly(Man-TMS) against Con A was evident. Comparing the amount of BSA immobilized on the poly(Man-*r*-TMS)-immobilized and unmodified cells, nonspecific binding between poly(Man-*r*-TMS) and BSA was not detected. It is suggested that this inertness toward nonspecific binding of protein was attributable to hydrophilization of the surface by saccharide. Typically, saccharide-immobilized surfaces have been hydrophilized, resulting in prevention of nonspecific interactions between proteins and surfaces.[17,59−61] The surface immobilized with poly(Man-*r*-TMS) showed specific recognition for Con A as a result of both the inhibition of nonspecific interactions and the glyco-cluster effect.

The amount of Con A adsorbed (approximately 0.13 μmol/m^2) was small relative to the amount of Man units immobilized (approximately 36 μmol/m^2, estimated from the copolymer composition). It is predicted that the copolymer is accumulated via condensation between TMS units in the copolymer. Jon et al. reported that aggregation of TMS-containing copolymer with a height of 5 nm was observed, depending on surface conditions.[41] In our research, Man units lying on the superficial layer should be predominant as the binding site with Con A.

To confirm the specificity of the poly(Man-*r*-TMS)-immobilized sensor cell to Con A, Con A was associated with Man before injection into the sensor cell. The relative ΔF_{max} of Man-pretreated Con A is shown in Figure 5. In the range to an equivalence of 10^3, the relative ΔF_{max} decreased with increasing equivalence molar ratio of Man. At an equivalence of 10^4, an increment of the relative ΔF_{max},

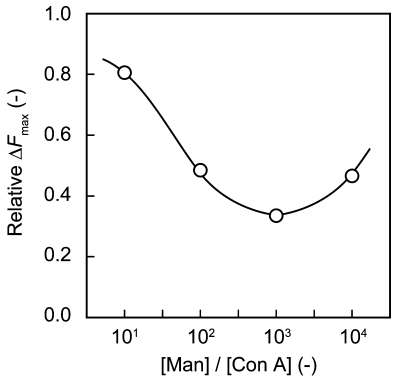

Figure 5. Relative ΔF_{max} of Man-pretreated Con A on poly(Man-*r*-TMS)-immobilized cell at the various equivalence molar ratios of Man.

presumably arising from nonspecific interaction between saccharides, was detected. The decreasing behavior of the relative ΔF_{max} with the molar ratio of Man indicated specific interaction between Con A and the Man residues in poly(Man-*r*-TMS).

3.3. Affinity Separation of Protein Using Poly(Man-*r*-TMS)-Immobilized Membrane. The obtained poly(AcMan-*r*-TMS) was immobilized on an inorganic porous membrane. The amount of poly(AcMan-*r*-TMS) immobilized was estimated to be 2.2 ± 1.0 mg/m^2 from the membrane weight before and after incubation in copolymer solution. The amount of AcMan residue contained in the copolymer immobilized on the membrane was 4.8 μmol/m^2. Immobilization of the poly(AcMan-*r*-TMS) on the membrane was confirmed by XPS, as shown in Figure 6. In the C(1s) spectrum of the

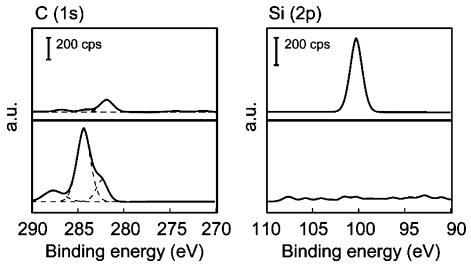

Figure 6. XPS spectra of the SPG membrane surface before and after immobilization of poly (AcMan-*r*-TMS). Above, unmodified membrane; below,: poly (AcMan-*r*-TMS)-immobilized membrane.

poly(AcMan-*r*-TMS)-immobilized membrane, peaks were observed at 283.9 and 287.0 eV, which correspond to C−C and C═O bonds, respectively. The C(1s) peak of the unmodified surface was weaker than that of the copolymer-modified surface. The peak corresponding to Si−O bonding (100.2 eV) was not present in the Si(2p) spectrum of the poly(AcMan-*r*-TMS)-immobilized membrane. These results suggest that the surface was mostly covered by the copolymer. The SPG membrane has a large number of penetrating pores.[62] The surfaces of the poly(AcMan-*r*-TMS)-immobilized membrane were examined by SEM (Figure 7). Pores in the range 1000−2000 nm were observed, with a wide distribution in the surfaces grafted with poly(AcMan-*r*-TMS), and the SEM images indicate that the porous structure of the membrane was maintained after immobilization of the copolymer. Use of a membrane with micrometer-order pores prevented protein size exclusion. The poly(Man-*r*-TMS)-immobilized membrane is expected to be an effective device for continuous bioseparation of pathogens.

The breakthrough curves and amounts of protein adsorbed during permeation of protein solutions through the unmodified or poly(Man-*r*-TMS)-immobilized membranes are shown in Figure 8. The adsorption behaviors agreed closely with the QCM results, showing that poly(Man-*r*-TMS) was barely bound to BSA but strongly adsorbed Con A. The breakthrough point of Con A through the poly(Man-*r*-TMS)-immobilized membrane was determined to be about 15 mL; otherwise, breakthroughs took place just after the start of permeation. The amount of Con A adsorbed on the poly(Man-*r*-TMS)-immobilized membrane was 34 nmol/m^2 and that on the SPG membrane was 0.33 nmol/m^2. On the other hand, the amounts of BSA adsorbed on both SPG membrane and poly(Man-*r*-TMS)-immobilized membrane were around 4.2 nmol/m^2. The amount of Con A adsorbed on the poly(Man-*r*-TMS)-immobilized membrane was less than that on the poly(Man-*r*-TMS)-immobilized cell; this was attributed to the diffusion-limited access of Con A continuously permeated in the membrane pores.

When Con A and BSA solutions were permeated through the unmodified membrane, most of the proteins passed into the effluent solution. Because the surface of the SPG membrane consists of multiple silanol groups, the innate hydrophilic surface prevented nonspecific interactions with proteins. After immobilizing poly(Man-*r*-TMS) on the membrane, the amount of Con A adsorbed was increased through the affinity of Man against Con A. In contrast, BSA was not adsorbed on the surface of the poly(Man-*r*-TMS)-immobilized membrane due to the inertness of the surface toward protein adhesion. SEM images of the poly(Man-*r*-TMS)-immobilized membrane and the passage of most of the BSA through the poly(Man-*r*-TMS)-immobilized membrane show that the mechanism for Con A removal is not by size exclusion, but by affinity adsorption. The affinity adsorption of Con A and the prevention of nonspecific adhesion on the poly(Man-*r*-TMS)-immobilized surface enabled selective bioseparation.

To elute the adsorbed Con A, we permeated Milli-Q water and a *p*NP-Man aqueous solution through the poly(Man-*r*-TMS)-immobilized membrane (Figure 9). In the case of water permeation, 15% of the adsorbed Con A was eluted because of the absence of calcium and magnesium ions. A high-concentration *p*NP-Man aqueous solution enabled the recovery of approximately half of the adsorbed Con A. The rest of the adsorbed Con A was remained because interactions between Con A and poly(Man-*r*-TMS) were not broken, as a result of the glyco-cluster effect. This elution could be caused by the lack of calcium and magnesium ions, affinity between Con A and the Man, excessive amounts of *p*NP-Man, and hydrophobic interactions via phenyl groups. Therefore, it is concluded that a poly(Man-*r*-TMS)-immobilized membrane is effective not only as a bioremoval material but also as a biopurification material.

Dansyl-Con A was adsorbed on the poly(Man-*r*-TMS)-immobilized membrane in coexistence with FITC-BSA. The relative concentrations of dansyl-Con A and FITC-BSA in the effluent solution through the poly(Man-*r*-TMS)-immobilized membrane are shown in Figure 10. When fluorescent-labeled proteins were permeated through the poly(Man-*r*-TMS)-immobilized membrane, 30% of FITC-BSA was captured on the poly(Man-*r*-TMS)-immobilized membrane, while 70% of dansyl-Con A was captured on the membrane. Con A is adsorbed on the poly(Man-*r*-TMS)-immobilized membrane

dx.doi.org/10.1021/am2014713 | *ACS Appl. Mater. Interfaces* 2012, 4, 411−417

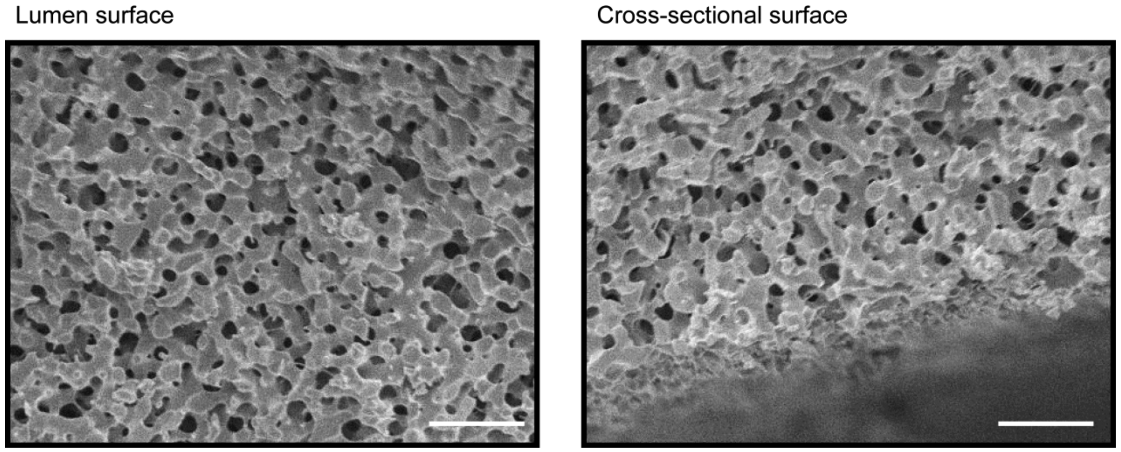

Figure 7. SEM image of the lumen and cross-sectional surface immobilized with poly (AcMan-*r*-TMS). Scale bars: 10 μm.

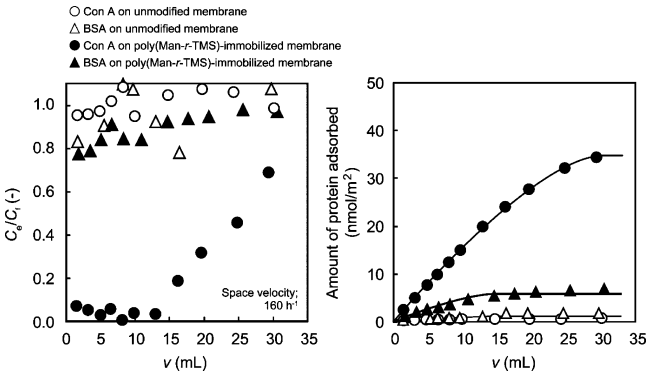

Figure 8. Breakthrough curve and amount of protein adsorbed on unmodified or poly(Man-*r*-TMS)-immobilized membranes.

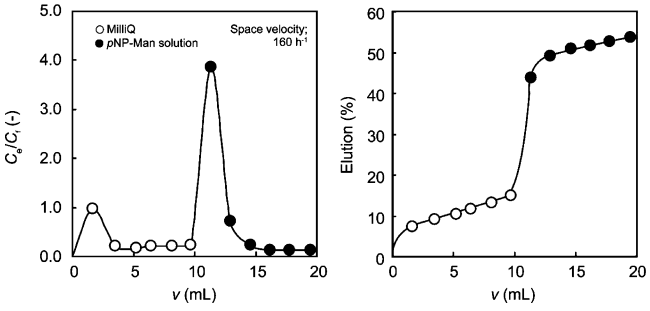

Figure 9. Elution curve and amount of Con A recovered from the poly(Man-*r*-TMS)-immobilized membrane.

through three steps: (1) convective transport of Con A in the pore, (2) diffusive transfer of Con A to the vicinity of immobilized poly(Man-*r*-TMS), and (3) binding of Con A with Man residues in poly(Man-*r*-TMS). The remaining dansyl-Con A was eluted from the membrane pores as a result of association of dansyl-Con A with FITC-BSA, increasing diffusive transfer resistance of Con A, and hindrance of dansyl group on the incorporation of Man residues at binding sites of Con A, using fluorescent-labeled proteins. The breakthrough curve indicates that dansyl-Con A was preferentially adsorbed on the membrane, compared with FITC-BSA. It is expected that Con A is selectively separated in the coexistent system using the poly(Man-*r*-TMS)-immobilized membrane by control of the space velocity.

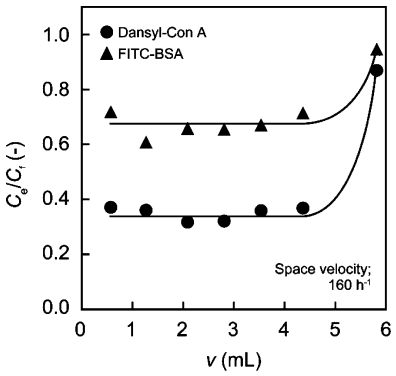

Figure 10. Relative concentration of dansyl-Con A and FITC-BSA in effluent solution through poly (Man-*r*-TMS)-immobilized membrane in the coexistent system.

4. CONCLUSION

A glycopolymer containing α-D-mannose was readily immobilized on the surface of materials by introduction of a silane coupling reagent within a copolymer. Poly(Man-*r*-TMS)-containing materials exhibited a high and specific recognition ability for lectin because of the glyco-cluster effect.

The results indicate that the glycopolymer-immobilized porous materials have further potential for removal of small pathogens, based on affinity purification, because various pathogens are transmitted via interaction with saccharide on the cell surface. We believe that this glyco-technology can be practically applied to pathogen-removal devices in fields of medical treatment and environmental detoxification.

■ ASSOCIATED CONTENT

Ⓢ Supporting Information

^{1}H NMR spectra and contact angle images. This material is available free of charge via the Internet at http://pubs.acs.org.

■ AUTHOR INFORMATION

Corresponding Author

*Tel: +81-92-802-2749. Fax: +81-92-802-2769. E-mail: miuray@chem-eng.kyushu-u.ac.jp.

■ ACKNOWLEDGMENTS

This work was supported by a Grant-in-Aid for Scientific Research on Innovative Areas (20106003).

REFERENCES

(1) Taylor, M. E.; Drickamer, K. In *Introduction to Glycobiology*; Oxford University Press: Oxford, U.K., 2003.
(2) Lee, C. Y.; Lee, T. R. *Acc. Chem. Res.* **1995**, *28*, 321−327.
(3) Mammen, M.; Choi, S.-K.; Whitesides, M. G. *Angew. Chem., Int. Ed.* **1998**, *37*, 2754−2794.
(4) Miura, Y.; Ikeda, T.; Kobayashi, K. *Biomacromolecules* **2003**, *4*, 410−415.
(5) Miura, Y.; Ikeda, T.; Wada, N.; Kobayashi, K. *Green Chem.* **2003**, *5*, 610−614.
(6) Miura, Y.; Ikeda, T.; Wada, N.; Kobayashi, K. *Macromol. Biosci.* **2003**, *3*, 662−667.
(7) Miura, Y.; Sato, H.; Ikeda, T.; Sugimura, H.; Takai, O.; Kobayashi, K. *Biomacromolecules* **2004**, *5*, 1708−1713.
(8) Miura, Y.; Wada, N.; Nishida, Y.; Mori, H.; Kobayashi, K. *J. Polym. Sci., Part A: Polym. Chem.* **2004**, *42*, 4598−4606.
(9) Miura, Y.; Koketsu, D.; Kobayashi, K. *Polym. Adv. Technol.* **2007**, *18*, 647−651.
(10) Miura, Y.; Yasuda, K.; Yamamoto, K.; Koike, M.; Nishida, Y.; Kobayashi, K. *Biomacromolecules* **2007**, *8*, 2129−2134.
(11) Sato, H.; Miura, Y.; Saito, N.; Kobayashi, K.; Takai, O. *Biomacromolecules* **2007**, *8*, 753−756.
(12) Miura, Y.; You, C.; Ohnishi, R. *Sci. Technol. Adv. Mater.* **2008**, *9*, 24407−24412.
(13) Fukuda, T.; Onogi, S.; Miura, Y. *Thin Solid Films* **2009**, *518*, 880−888.
(14) Toyoshima, M.; Miura, Y. *J. Polym. Sci., Part A: Polym. Chem.* **2009**, *47*, 1412−1421.
(15) Fukuda, T.; Matsumoto, E.; Onogi, S.; Miura, Y. *Bioconjugate Chem.* **2010**, *21*, 1079−1086.
(16) Miura, Y.; Mizuno, H. *Bull. Chem. Soc. Jpn.* **2010**, *83*, 1004−1009.
(17) Toyoshima, M.; Oura, T.; Fukuda, T.; Matsumoto, E.; Miura, Y. *Polym. J.* **2010**, *42*, 172−178.
(18) Ishii, J.; Toyoshima, M.; Chikae, M.; Takayura, Y.; Miura, Y. *Bull. Chem. Soc. Jpn.* **2011**, *84*, 466−470.
(19) Merritt, A. E.; Sarfaty, S.; Vandenakker, F.; Lhoir, C.; Martial, A. J.; Hol, J. G. W. *Protein Sci.* **1994**, *3*, 166−175.
(20) Hammache, D.; Piéroni, G.; Yahi, N.; Delézay, O.; Koch, N.; Lafont, H.; Tamalet, C.; Fantini, J. *J. Biol. Chem.* **1998**, *27*, 7967−7971.
(21) Schilling, D. J.; Mulvey, A. M.; Hultgren, J. S. *J. Infect. Dis.* **2001**, *183*, S36−40.
(22) Kim, M.; Saito, K.; Furusaki, S.; Sugo, T.; Ishigaki, I. *J. Chromatogr.* **1991**, *586*, 27−33.
(23) Ritter, K. *J. Immunol. Methods* **1991**, *137*, 209−215.
(24) Beeskow, C. T.; Kusharyoto, W.; Anspach, B. F.; Kroner, H. K.; Deckwer, D. W. *J. Chromatogr., A* **1995**, *715*, 49−65.
(25) Kubota, N.; Nakagawa, Y.; Eguchi, Y. *J. Appl. Polym. Sci.* **1996**, *62*, 1153−1160.
(26) Guo, W.; Shang, Z.; Yu, Y.; Zhou, L. *Biomed. Chromatogr.* **1997**, *11*, 164−166.
(27) Ruckenstein, E.; Zeng, F. X. *J. Membr. Sci.* **1998**, *142*, 13−26.
(28) Zeng, X.; Ruckenstein, E. *J. Membr. Sci.* **1999**, *156*, 97−107.
(29) Frazier, A. R.; Matthijs, G.; Davies, C. M.; Roberts, J. C.; Schacht, E.; Tendler, B. J. S. *Biomaterials* **2000**, *21*, 957−966.
(30) Huang, M.; Shen, Z.; Zhang, Y.; Zeng, X.; Wang, G. P. *Bioorg. Med. Chem. Lett.* **2007**, *17*, 5379−5383.
(31) Ortega-Munoz, M.; Lopez-Jaramillo, J.; Hernandez-Mateo, F.; Santoyo-Gonzalez, F. *Adv. Synth. Catal.* **2006**, *348*, 2410−2420.
(32) Santoyo-Gonzalez, F.; Hernandez-Mateo, F. *Chem. Soc. Rev.* **2009**, *38*, 3449−3462.
(33) Moni, L.; Ciogli, A.; D'Acquarica, I.; Dondoni, A.; Gasparrini, F.; Marra, A. *Chem.—Eur. J.* **2010**, *16*, 5712−5722.
(34) Huang, L.; Dolai, S.; Raja, K.; Kruk, M. *Langmuir* **2010**, *26*, 2688−2693.
(35) Narla, N. S.; Sun, L.-X. *Org. Biomol. Chem.* **2011**, *9*, 845−850.
(36) Weetall, H. H.; Hersh, S. L. *Biochim. Biophys. Acta, Enzymol.* **1969**, *185*, 464−465.
(37) Weetall, H. H. *Biochim. J.* **1970**, *177*, 257−261.
(38) Balachander, N.; Sukenik, N. C. *Langmuir* **1990**, *6*, 1621−1627.
(39) Pope, M. N.; Kulcinski, L. D.; Hardwick, A.; Chang, Y.-A. *Bioconjugate Chem.* **1993**, *4*, 166−171.
(40) Park, S. Y.; Ito, Y.; Imanishi, Y. *Macromolecules* **1998**, *31*, 2606−2610.
(41) Khademhosseini, A.; Jon, S.; Suh, Y. K.; Tran, T. T.-N.; Eng, G.; Yeh, J.; Seong, J.; Langer, R. *Adv. Mater.* **2003**, *15*, 1995−2000.
(42) Jon., S.; Seong, J.; Khademhosseini, A.; Tran, T. T.-N.; Laibinis, E. P.; Langer, R. *Langmuir* **2003**, *19*, 9989−9993.
(43) Grigoropoulou, G.; Stathi, P.; Karakassides, A. M.; Louloudi, M.; Deligiannakis, Y. *Colloids Surf., A* **2008**, *320*, 25−35.
(44) Wang, H.-J.; Zhou, W.-H.; Yin, X.-F.; Zhuang, Z.-X.; Yang, H.-H.; Wang, X.-R. *J. Am. Chem. Soc.* **2006**, *128*, 15954−15955.
(45) Jana, R. N.; Earhart, C.; Ying, Y. J. *Chem. Mater.* **2007**, *19*, 5074−5082.
(46) Kim, J. E.; Shin, H.-Y.; Park, S.; Sung, D.; Jon, S.; Sampathkumar, S.-G.; Yarema, J. K.; Choi, S.-Y.; Kim, K. *Chem. Commun.* **2008**, 3543−3545.
(47) Shah, S. S.; Howland, C. M.; Chen, L. J.; Silangcruz, J.; Verkhoturov, V. S.; Schweikert, A. E.; Parikh, N. A.; Revzin, A. *ACS Appl. Mater. Interfaces* **2009**, *1*, 2592−2601.
(48) SelegÅrd, L.; Khranovskyy, V.; Sderlind, F.; Vahlberg, C.; Ahrn, M.; Kll, P.-O.; Yakimova, R.; Uvdal, K. *ACS Appl. Mater. Interfaces* **2010**, *2*, 2128−2135.
(49) Ritchie, C. M. S.; Bachas, G. L.; Olin, T.; Sikdar, K. S.; Bhattacharyya, D. *Langmuir* **1999**, *15*, 6346−6357.
(50) Abdelmouleh, M.; Boufi, S.; Salah, B. A.; Belgacem, N. M.; Gandini, A. *Langmuir* **2002**, *18*, 3203−3208.
(51) Hattori, K.; Hiwatari, M.; Iiyama, C.; Yoshimi, Y.; Kohori, F.; Sakai, K.; Piletsky, S. A. *J. Membr. Sci.* **2004**, *233*, 169−173.
(52) Li, S.; Zhang, S.; Wang, X. *Langmuir* **2008**, *24*, 5585−5590.
(53) Lis, H.; Sharon, N. *Chem. Rev.* **1998**, *98*, 637−674.
(54) Ebara, Y.; Itakura, K.; Okahata, Y. *Langmuir* **1996**, *12*, 5165−5170.
(55) Bradford, M. M. *Anal. Biochem.* **1976**, *72*, 248−254.
(56) Varma, K. I.; Tomar, K. A.; Anand, C. R. *J. Appl. Polym. Sci.* **1987**, *33*, 1377−1388.
(57) Goldstein, J. I.; Hollerman, E. C.; Smith, E. E. *Biochemistry* **1965**, *4*, 876−883.
(58) Mandal, K. D.; Kishore, N.; Brewer, F. C. *Biochemistry* **1994**, *33*, 1149−1156.
(59) Prime, L. K.; Whitesides, M. G. *Science* **1991**, *252*, 1164−1167.
(60) Seto, H.; Ohto, K.; Kawakita, H. *J. Membr. Sci.* **2011**, *370*, 76−81.
(61) Wang, Y.; El-Boubbou, K.; Kouyoumdjian, H.; Sun, B.; Huang, X.; Zeng, X. *Langmuir* **2010**, *26*, 4199−4125.
(62) Kawakita, H.; Seto, H.; Ohto, K.; Inoue, K.; Harada, H. *Biochem. Eng. J.* **2007**, *36*, 190−193.